JOURNAL OF Materials CHEMISTRY

Intercalation of alkylammonium cations into expandable fluorine mica and its application for the evaluation of heterogeneous charge distribution

Jae-Hun Yang,[a] Yang-Su Han,[a] Jin-Ho Choy*[a] and Hiroshi Tateyama[b]

[a]*National Nanohybrid Materials Laboratory(NNML), School of Chemistry and Molecular Engineering, Seoul National University, Seoul 151-747, Korea. E-mail: jhchoy@plaza.snu.ac.kr; Fax: +82-2-872-9864; Tel: +82-2-880-6658*

[b]*Kyushu National Industrial Research Institute, Suku-machi, Tosu city, Saga Prefecture, 841, Japan*

Received 26th July 2000, Accepted 4th December 2000
First published as an Advance Article on the web 2nd February 2001

The interstratified layer nano-hybrids between n-alkylammonium and fluorine mica are prepared by ion-exchanging the interlayer Na^+ ions in the synthetic fluorine mica, $Na_{0.66}Mg_{2.68}(Si_{3.98}Al_{0.02})O_{10.02}F_{1.96}$, with n-alkylammonium cations, $CH_3(CH_2)_{n-1}NH_3^+$ (C_n; $n=6$, 8, 10, 12, 14, 16, and 18). According to the X-ray diffraction profiles of nano-hybrids and their computer simulation results, their interstratified structural features could be clearly distinguished depending upon the number of carbon atoms in the alkyl chain (C_n). The C_6–C_8 and C_{14}–C_{16} derivatives exhibit normal intercalation phases with the basal spacings of $\sim$13.8 Å and $\sim$18.0 Å, indicating the parallel mono- and bilayer arrangements of the intercalants between silicate layers, respectively. On the other hand, the C_{10}–C_{12} and C_{18} hybrids show distinct superlattice lines in the X-ray diffraction patterns due to the interstratification between parallel monolayer–bilayer ($d_{001}=31.6$ Å) and parallel bilayer–pseudotriple layer ($d_{001}=39.6$ Å) of alkylammonium molecules, respectively, in the interlayer space of mica. The origin of such interstratification is found to be due to the charge heterogeneity of silicate interlayers in the Na^+-fluorine mica; a high layer charge with 0.37 e^-/Si_4O_{10} and a low one with 0.28 e^-/Si_4O_{10} charge densities, respectively. The charge heterogeneity of silicate layers is also confirmed through the step-wise deintercalation of intercalants during their thermolysis under a nitrogen atmosphere.

Introduction

Layered silicates, in particular, with 2 : 1 mica-type structures, possess diverse intercalation properties, and therefore have been widely studied for a variety of materials applications including catalysts and catalyst supports, ion exchangers, adsorbents, and inorganic functional additives.[1–3] In recent years, they have become of special interest as ideal inorganic hosts in constructing layered hybrids with specific functions.[4–6] Since the structures and physico-chemical properties of nano-hybrids based on layered silicates strongly depend not only on the nature of the gallery species but also on the characteristics of the inorganic layers, such as the interlayer charge density and its distribution, it is very important to understand the layer characteristics in designing and constructing nano-hybrids with desired physico-chemical properties.[7]

Recently, Na^+-fluorine mica with a comparable swelling property to that of natural smectites has been successfully synthesized by a solid state intercalation route.[8,9] The synthetic mica, unlike natural ones, is highly crystalline, controllable in composition, highly pure and optically transparent. It is, therefore, quite advantageous to employ the synthetic mica as an inorganic matrix in the construction of functional layered nanocomposites. Furthermore, the synthetic Na-fluorine mica displays unique interstratification behavior upon ion exchange and/or pillaring of gallery species owing to the heterogeneous charge distribution from layer to layer in a highly ordered manner,[10] offering a way of designing and constructing novel heterostructured layer materials with high synergism. For instance, rectorite-like pillared compounds obtained by ion exchange of Mg^{2+} in a controlled manner and subsequent pillaring of Al_2O_3 exhibit excellent hydrothermal and thermal stabilities, porosity and good catalytic activities.[11] In spite of the promising features of synthetic micas as inorganic matrices, there have been few studies on their intercalation chemistry.[12]

In the present study, therefore, our primary attention was aimed at understanding the intercalation behavior of synthetic Na^+-fluorine mica on the basis of the interlayer charge density and its distribution. For this purpose, n-alkylammonium molecules with a variable chain length are intercalated into synthetic fluorine mica, and the interlayer structures of the complexes and the intercalation/deintercalation processes are fully discussed on the basis of the interlayer charge density, layer stacking sequence, and charge distribution of the Na^+-fluorine mica.

Experimental

Sample preparation

The starting layered silicate used in this study was a synthetic Na^+-fluorine mica (Na-M) with the chemical formula $Na_{0.66}Mg_{2.68}(Si_{3.98}Al_{0.02})O_{10.02}F_{1.96}$ (ME-100, CO-OP Chemicals) and an average particle size of 1.2 μm. The cation exchange capacity (CEC) of the mica was estimated to be 84.9 meq (100 g)$^{-1}$ from the total elemental analysis,[10] but to be 115 meq (100 g)$^{-1}$ when the methylene blue adsorption method was employed.[13] n-Alkylammonium chlorides with different chain lengths, $[CH_3(CH_2)_{n-1}NH_3]^+Cl^-$, C_nCl ($n=6$, 8, 10, 12, 14, 16, and 18), were used as intercalants. Organo-mica hybrids

DOI: 10.1039/b006059n

were prepared by conventional ion exchange reaction. In a typical preparation, sodium fluorine mica (1 g) was dispersed in 100 ml deionized water, then n-alkylammonium chlorides (3 times the CEC of the mica; 84.9 meq (100 g)$^{-1}$) were added to the clay suspension, and reacted at 65 °C under continuous stirring. In order to achieve the complete replacement of the interlayer Na^+ ions with the gallery species, the ion-exchange reaction was extended up to 192 h (8 days) with refreshing the reaction solutions every day. The final reaction products were separated by centrifugation and washed thoroughly with a mixed solution of ethanol and water (about 50% vol/vol).

Characterization

Powder X-ray diffraction (XRD) patterns were taken on the sample spread on a glass slide using a Phillips PW1830 diffractometer equipped with Ni-filtered Cu-Kα radiation ($\lambda = 1.5418$ Å). The diffraction data were collected using a step-scanning speed of 0.02° 2θ per second. Simultaneous thermogravimetry (TG)–differential thermal analysis (DTA) was performed for the air dried samples under a nitrogen atmosphere with a heating rate of 5 °C min^{-1} using a Rigaku TAS-100 thermal analyzer. The evolutions of interlayer structures during thermolysis were also monitored by XRD for the samples thermally treated under a nitrogen atmosphere at the temperatures pre-determined from the TG analysis.

Calculation of X-ray diffraction patterns

For interstratified or mixed-layer structures in which two or more kinds of unit layers are arranged regularly or irregularly along the *c*-axis direction, it is very useful to compare the observed intensity with the theoretical one calculated from a structural model. In the present study, the theoretical X-ray diffraction profiles for interstratified structures were obtained by applying Kakinoki and Komura's equation[14,15] based on the structural model shown in Fig. 1.

In the theoretical calculation, the integrated intensity for an interstratified crystal consisting of N layers and n types of layers can be expressed as follows:

$$I = N\mathrm{Spur}(VF) + \sum_{n=1}^{N-1}(N-n)\mathrm{Spur}(VFQ^n) + \mathrm{conj.} \qquad (1)$$

where Spur means the sum of the diagonal elements of square matrix, and conj. the complex conjugate of the foregoing terms. The symbols in eqn. (1) are

$$V = \begin{bmatrix} V_1 * V_1 & V_1 * V_2 & \cdots & V_1 * V_R \\ V_2 * V_1 & V_2 * V_2 & \cdots & V_2 * V_R \\ \vdots & \vdots & \vdots & \vdots \\ V_R * V_1 & V_R * V_2 & \cdots & V_R * V_R \end{bmatrix}_R \quad F = \begin{bmatrix} W_1 & 0 & \cdots & 0 \\ 0 & W_2 & \cdots & 0 \\ \vdots & \vdots & \vdots & \vdots \\ 0 & 0 & \cdots & W_R \end{bmatrix}_R$$

$$P = \begin{bmatrix} P_{11} & P_{12} & \cdots & P_{1R} \\ P_{21} & P_{22} & \cdots & P_{2R} \\ \vdots & \vdots & \vdots & \vdots \\ P_{R1} & P_{R2} & \cdots & P_{RR} \end{bmatrix}_R \qquad (2)$$

$$\Phi = \begin{bmatrix} \exp(-\Psi_1) & 0 & \cdots & 0 \\ 0 & \exp(-\Psi_2) & \cdots & 0 \\ \vdots & \vdots & \vdots & \vdots \\ 0 & 0 & \cdots & \exp(-\Psi_R) \end{bmatrix}_R$$

$$Q = \Phi P$$

where V is the matrix of structure factors for the layer, F is the matrix of existing probability, P is the matrix of transition probability of the layer to the next one, and Φ is the matrix of phase factors, respectively. The intensity was calculated by multiplying by the powder Lorentz and polarization (Lp) factor. In this study, the number of component layers, N, was fixed to be $N = 10$ and its standard deviation $\sigma = 2.0$, which is a usual mean value for smectites.[16] For an interstratified system with two kinds of layers (i layer and j layer) and Reichweite $g = 1$, the relationships between proportions of the different kinds of layers and probabilities are given by :

$$\begin{aligned} W_i + W_j &= 1 \\ P_{ii} + P_{ij} &= 1 \\ P_{ji} + P_{jj} &= 1 \\ W_i \cdot P_{ij} &= W_j \cdot P_{ji} \end{aligned} \qquad (3)$$

Of these, the independent variables are W_i and P_{ij}, because for given values of W_i and P_{ij}, other parameters become fixed.

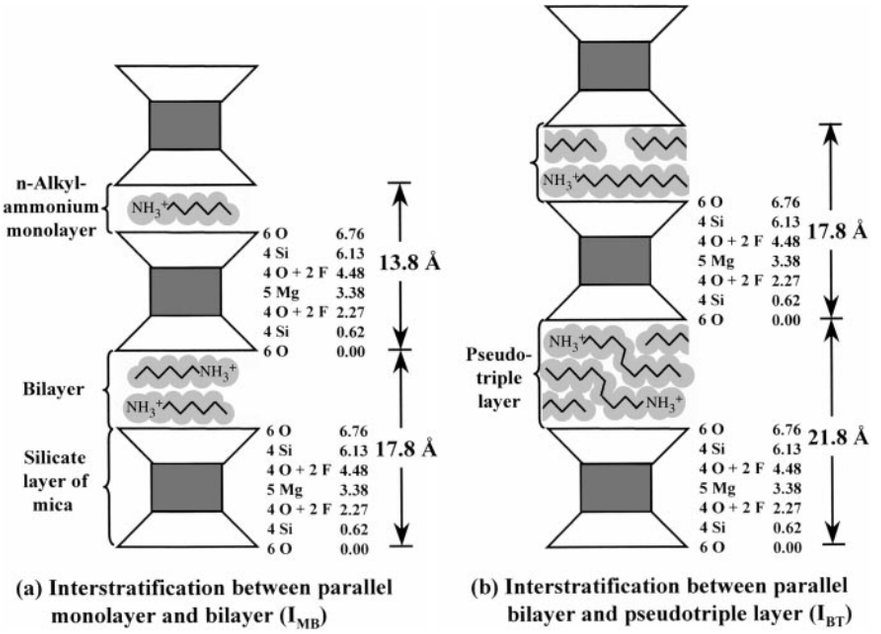

(a) Interstratification between parallel monolayer and bilayer (I_{MB})

(b) Interstratification between parallel bilayer and pseudotriple layer (I_{BT})

Fig. 1 Structural model used in the calculation of powder X-ray diffraction patterns.

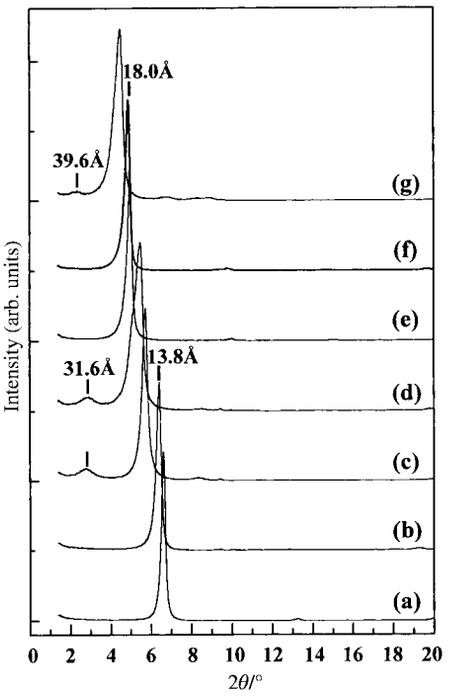

Fig. 2 Evolution of powder X-ray diffraction patterns for the alkylammonium-mica hybrids depending upon the number of carbons (C_n); (a) C_6-M, (b) C_8-M, (c) C_{10}-M, (d) C_{12}-M, (e) C_{14}-M, (f) C_{16}-M, and (g) C_{18}-M.

Results and discussion

Powder X-ray diffraction

As well documented,[1,2] alkylammonium molecular ions are easily intercalated into silicate layers of mica to form organo-mica hybrids. Fig. 2 shows the evolution of XRD patterns for the layer hybrids as a function of the number of carbons in the alkyl chain. The basal spacings (d_{001}) of C_6- and C_8-M complexes ((a) and (b)) are ~13.4 Å and ~13.8 Å respectively, indicating that the intercalated alkylammonium cations are oriented parallel to the basal plane of the silicate layers. As the alkyl chain length increases to C_{10} (c), an additional weak (001) reflection at $2\theta = 2.79°$ ($d_{001} = 31.6$ Å) appears, which can be assigned to a superlattice line due to the interstratification between parallel monolayers with a thickness of 13.8 Å and parallel bilayers of 17.8 Å (I_{MB}) (Fig. 1(a) and Fig. 5(b)—see later). The observed XRD profile for the C_{12}-M hybrid (d) shows also a long-spacing reflection at 31.6 Å, which is identical with that of C_{10}-M. Thus, the interstratified structure of C_{12}-M can be interpreted as a regular interstratification of 13.8 Å monolayers and 17.8 Å bilayers. However, the (002) reflection at 5.46° is quite broad and asymmetric and the basal reflection is displaced compared with that of C_{10}-M, implying that some of the 13.8 Å layers are transformed into 17.8 Å bilayers. As the carbon number in the alkyl chain increases further to C_{14} and C_{16} ((e) and (f)), the superlattice lines due to superstructure disappear, but the normal intercalation phases with the basal spacings of ~18.0 Å are observed, which indicates the formation of parallel bilayers of alkylammonium molecules between the silicate layers. Another interstratified phase (I_{BT}) appears in the C_{18}-M hybrid (g), where the (001) reflection at 39.6 Å is assignable to the superstructure of the parallel bilayer structure (17.8 Å) and pseudo-triple layer structure (21.8 Å)[7] (Fig. 1(b) and Fig. 5(d)—see later).

Quantification of interstratified structure

In order to obtain more detailed information on the layer stacking for the two different types of interstratified structures

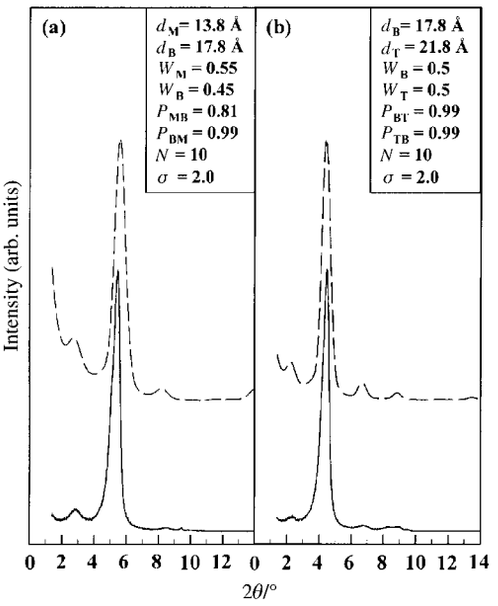

Fig. 3 Comparison of experimental (solid line) and calculated (dashed line) powder X-ray diffraction patterns of interstratified samples; (a) C_{10}-M and (b) C_{18}-M. The best fitted simulation parameters are summarized in the insets, respectively.

(I_{MB} and I_{BT}), the observed powder X-ray diffraction profiles are simulated with the general intensity equation proposed by Kakinoki and Komura as described before. Fig. 3 compares the observed X-ray diffraction patterns with the calculated ones, and the best fitted parameters are also summarized in the insets. The observed XRD pattern for C_{10}-M (a) is well consistent with the calculated one, assuming that the superstructure consists of 13.8 Å parallel monolayers and 17.8 Å parallel bilayers. The existing probabilities of the former (W_M) and the latter (W_B) are estimated to be 0.55 and 0.45, respectively, and the transition probabilities of $P_{MB} = 0.81$ and $P_{BM} = 0.99$ are obtained. These results support again that the intercalated ammonium molecules are arranged differently between silicate layers depending upon the layers owing to the difference in the layer charge. Furthermore, the two differently charged layers (high-charge and low-charge layers) are quite regularly alternated along the *c*-axis.

For the C_{18}-M hybrid (b), the observed X-ray diffraction profile also shows good agreement with the calculated one when the simulation parameters, $W_B = 0.5$, $W_T = 0.5$, $P_{BT} = 0.99$, and $P_{TB} = 0.99$, are assumed. Thus, the superstructure observed in the C_{18}-M hybrid can be ascribed to the regular interstratification between the parallel bilayer (17.8 Å) and the pseudotriple layer (21.8 Å) arrangement of interlayer alkylammonium molecules. From the computer simulation for the interstratified structures, it can be concluded that the synthetic Na^+-fluorine mica possesses two kinds of interlayers with different cationic charge densities, those which are highly ordered along the *c*-axis.

Interlayer charge density

In characterizing clay minerals, including synthetic mica, the layer charge is particularly important because it determines the cation retention capacity or CEC, adsorption selectivity, swelling property, and interlayer structures of intercalants. The simplest way of estimating the layer charge might be the total elemental analysis of clay samples.[17,18] However, this does not reflect the effective layer charge because it includes the effects not only from the layer itself but also from the lateral edges of clay particles, and moreover it can not give any information on the charge heterogeneity within the layer. However, the alkylammonium method proposed by Lagaly

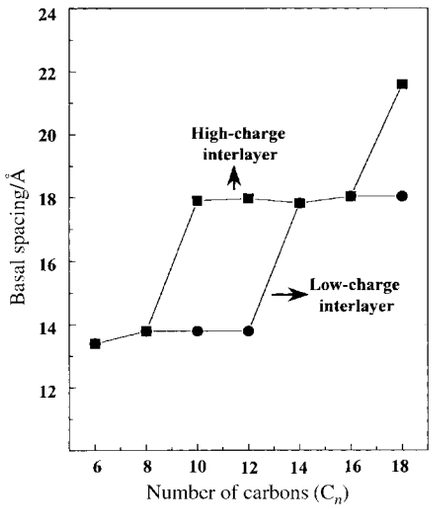

Fig. 4 Evolution of the basal spacing as a function of C_n.

and Weiss[7,19,20] offers a certain advantage since it provides a simple way to estimate the layer charge and at the same time to probe the charge heterogeneity in mixed layer clays from XRD analysis.

The layer charge of individual sheet in the Na^+-fluorine mica is, therefore, estimated with the n-alkylammonium method by measuring the basal spacings as a function of the number of carbon atoms in the alkyl chain (Fig. 4). The basal spacings of the interstratified phases are separated into the component layers based on simulation results, that is, the basal spacings of C_{10}- and C_{12}-M hybrids are regarded as the sum of individual layers with 13.8 Å and 17.8 Å thicknesses. Similarly, the basal spacing of C_{18}-M (39.6 Å) can be assigned as the sum of 1 : 1 interstratified layers with thicknesses of 17.8 Å and 21.8 Å. As shown in Fig. 4, a drastic increase in basal spacing could be observed at C_8–C_{10}, and also at C_{16}–C_{18} indicating the structural transition of the interlayer alkyl chains from monolayer to bilayer and also from bilayer to pseudotriple layer, respectively, in the high-charge layer. However, in the other layers with a low charge, a monolayer/bilayer transition is observed around C_{12} and C_{14}. Thus the layer charge for the individual layers can be calculated from the following equation:[7]

$$\frac{a\times b/2}{5.67C_n(I)+14}\leq\xi\leq\frac{a\times b/2}{5.67C_n(I')+14} \quad (4)$$

where a, b are cell parameters of Na^+-fluorine mica ($a=5.24$ Å and $b=9.08$ Å),[8] ξ is the layer charge density, $C_n(I)$ is the maximum carbon number in the monolayer arrangement, and $C_n(I')$ is the minimum carbon number in the bilayer arrangement.

In the case of highly charged layer, the maximum (ξ_{max}) and minimum (ξ_{min}) layer charges are calculated to be 0.41 and 0.34 e^-/Si_4O_{10}, respectively, leading to an average interlayer charge density (ξ_{avg}) of 0.37 e^-/Si_4O_{10}. Similarly, for the low-charge layer, the interlayer charge densities are estimated to be $\xi_{max}=0.29$, $\xi_{min}=0.26$, and $\xi_{avg}=0.28$ e^-/Si_4O_{10}, respectively. It is therefore concluded that the synthetic Na^+-fluorine mica is composed of two kinds of interlayers with different layer charges. In addition, Fig. 4 enables us to infer the charge distribution from the transition behavior. The sharp transitions of monolayer/bilayer and bilayer/pseudotriple layer reflect that the charge distributions within the layers are fairly homogeneous.[7]

Structure models of organo-mica hybrids

On the basis of the XRD and its simulation results, we are able to propose a possible structure model for the organo-mica hybrids as depicted in Fig. 5. In the intercalation compounds between clays and organic molecules, the interlayer structure is mainly governed by the layer charge of the clay and the dimensions of the guest species. Thus, in order to propose a reasonable interlayer structure, the steric limitations usually given by the equivalent area (A_e) of clay lattices and the area demand (A_c) of intercalated molecules should be taken into account. The equivalent area (A_e), the area available for a monolayer cation in the interlayer space, of the Na-fluorine mica can be estimated from the equation of $A_e=ab/2\xi$, where a and b are lattice parameters and ξ is the layer charge.[7] Thus the high- and low-charged layers provide areas of about 64 $Å^2$ and 88 $Å^2$ per unit charge, respectively, while the area demand for a n-alkylammonium molecule (A_c) is given by $A_c=5.67\times C_n+14$ ($Å^2$).[7] According to the relation, the C_6 and C_8 alkylammonium cations may need areas of 48.0 $Å^2$ and 59.4 $Å^2$ per molecule, respectively. Since A_c is sufficiently larger than A_e, the interlayer alkylammonium molecules form parallel monolayer arrangements in each gallery space of the high- and low-charged interlayers (Fig. 5(a)). If the area of flat-lying alkylammonium molecules is larger than the equivalent area, the monolayer rearranges into the bilayer to avoid the steric limitation. In the highly charged interlayer, therefore, C_{10} (70.7 $Å^2$) and C_{12} (82.0 $Å^2$) molecules form parallel bilayers

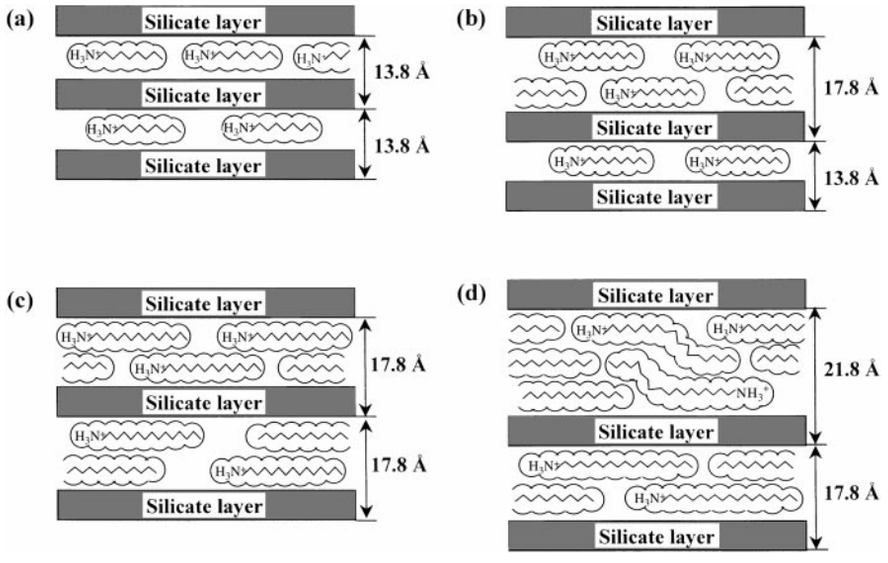

Fig. 5 Possible interlayer structure models of the alkylammonium intercalated micas.

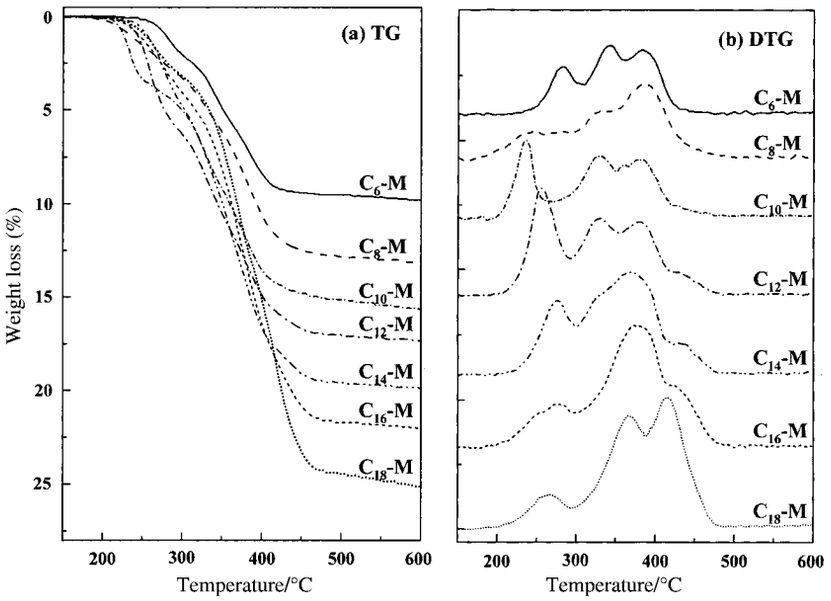

Fig. 6 (a) TG and (b) DTG curves for the alkylammonium intercalated fluorine mica hybrids.

with a basal spacing of ~17.8 Å, while the low-charged interlayers remain in a monolayer arrangement, which eventually results in the interstratification between the two layers (Fig. 5(b)). As the alkyl chain length increases to C_{14} and C_{16}, the A_c of alkylammonium molecules (93.4 $Å^2$ for C_{14} and 104.7 $Å^2$ for C_{16}) is larger than the equivalent area (A_e) of the base area of the low-charged interlayer (~88 $Å^2$), and therefore the parallel bilayer structure of the alkyl chain becomes more favorable in the interlayer space (Fig. 5(c)). Thus, the superlattice lines due to the interstratification disappear from the XRD pattern (Fig. 2(e) and (f)). With a further increase of the alkyl chain length to C_{18}, the area demand of the C_{18} molecule (116.1 $Å^2$) approaches the limiting base area for the parallel bilayer structure of alkyl chains in the highly charged layer (64.0 $Å^2 \times 2 = 128.0$ $Å^2$). In this situation, the individual chains are thought to adopt a hybrid arrangement with both lateral and paraffin-type segments leading to a pseudotriple layer with a basal spacing of ~22 Å. Eventually, the superstructure consists of regularly ordered bilayers (17.8 Å) and a pseudotriple layer (21.8 Å) can appear in the C_{18}-M hybrid (Fig. 5(d)).

Thermogravimetric analysis (TG)

A study on the thermal decomposition of alkylammonium cations intercalated in the silicate layers was also carried out to determine the intercalated alkylammonium content and the pathway of the specific decomposition reaction depending upon the layer charge. Fig. 6 represents the TG (a) and DTG curves (b), respectively. In order to investigate the structural evolutions of the intercalation compounds during thermolysis, XRD patterns for the samples heated at the temperatures predetermined from the TG analyses are also compared in Fig. 7.

Firstly, the content of intercalated ammonium molecules was estimated from the observed weight loss in the temperature range 150–600 °C, and the results are summarized in Table 1. Since the synthetic fluorine mica is composed of alternating layers of high ($\xi_{avg} = 0.37$ e^-/Si_4O_{10}) and low charge ($\xi_{avg} = 0.28$ e^-/Si_4O_{10}) with the mixing ratio of 1 : 1, the theoretical molar content of alkylammonium molecules stabilized in the interlayer space should be ~0.33 mol/Si_4O_{10}. Thus, the observed content is in an excess of 20–40% by mol and the deviation becomes obvious as the number of carbon atoms in the alkyl chain (C_n) increases. As the charge determined by n-alkylammonium methods provides information on the interlayer exchangeable sites only, it excludes the exchangeable cation sites residing at the crystal edges. For many aluminosilicates, however, the edge charge comprises about 20% of the total charges, but becomes significant as the particle size decreases.[7,21] In fact, the CEC of the synthetic fluorine mica estimated by the methylene blue adsorption method, which includes the contribution from edge sites as well as interlayer exchange ones, was found to be 115 meq (100 g)$^{-1}$.[13] This is an indication that the edge contribution exceeds ~35%, since the synthetic fluorine mica is prepared as fine powders with the average size of 1.2 μm. Moreover, additional alkylammonium cations exceeding the interlamellar exchange capacity would be adsorbed between the silicate layers through the van der Waals interaction between alkyl chains. Since the van der Waals attraction is proportional to the number of $-CH_2-$ groups (1–1.5 kJ per $-CH_2-$),[22] the effect becomes pronounced as the chain length increases. Therefore, in the case of C_{18}-M complexes, an additional van der Waals interaction between hydrophobic chains further increases the organic content.

Table 1 also suggests that all the interlayer Na^+ ions are not replaced quantitatively by the intercalants. About 35% of the interlayer Na^+ ions remain constant even when the reaction period is extended up to 8 days. Thus, the incomplete replacement of the interlayer Na^+ ions cannot be ascribed to simple insufficient saturation, but to the intrinsic chemical reactivity. In other words, there are two chemically non-equivalent Na^+ sites in the synthetic Na^+-fluorine mica; one is active for ion-exchange reactions, the other is not. This non-equivalence of Na^+ sites is suspected to be strongly correlated with the formation of interstratified structures in the alkylam-

Table 1 Thermal analysis results of n-alkylammonium-mica hybrids

Sample	Total weight loss[a](%)	Molar content, x[b]
C_6-M	9.6	0.39
C_8-M	12.8	0.43
C_{10}-M	15.3	0.43
C_{12}-M	16.9	0.42
C_{14}-M	19.6	0.43
C_{16}-M	21.7	0.44
C_{18}-M	24.6	0.46

[a]The values refer to the weight loss in the temperature range 150–600 °C. [b]The molar content was estimated from the total weight loss on the basis of the chemical formula, $(C_nNH_3^+)_x(Na)_{0.66-x}(Si_{3.98}Al_{0.02})O_{10.02}F_{1.96}$.

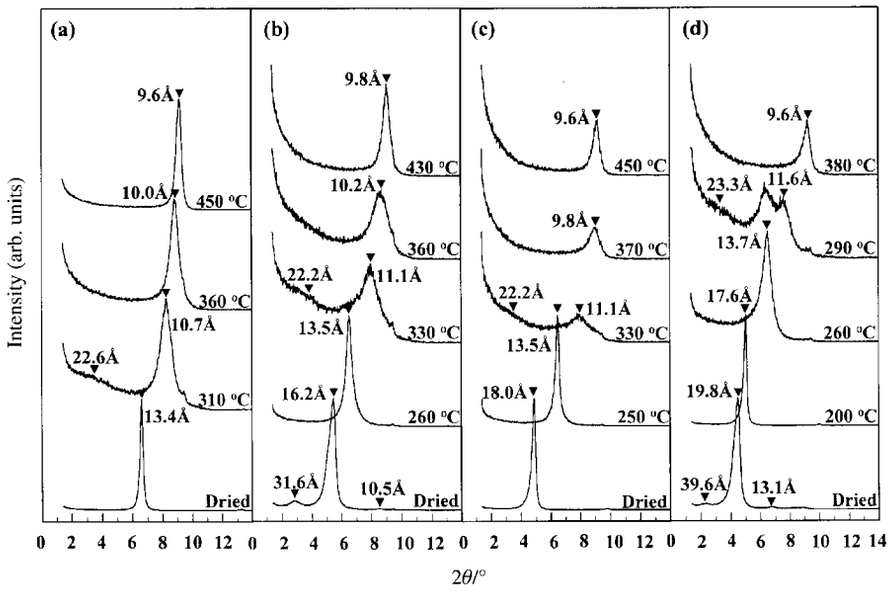

Fig. 7 Evolution of X-ray diffraction patterns of selected alkylammonium mica hybrids heated at the given temperatures. (a) C_6-M, (b) C_{10}-M, (c) C_{16}-M and (d) C_{18}-M.

monium-mica hybrids, which is again well consistent with our model calculation and XRD results.

Deintercalation

Thermal decomposition of alkylammonium mica hybrids takes place in several steps in the temperature range 150–500 °C under N_2 atmosphere. The thermogram of the C_6-M hybrid (Fig. 6(a) and (b)) shows three weight loss steps in the temperature ranges 220–310 °C, 310–365 °C, 365–450 °C, respectively. Correlating the first and the second weight loss steps with the layer charge of silicate layers, it is strongly believed that the peak around 220–310 °C is due to the desorption of organics from the low-charged layers and that of 310–365 °C from the high-charged layers. This consideration is reasonable since the ionic bonding character between C_6-ammonium ion and the negatively charged layer can be considered to be stronger in the highly charged interlayers. According to the previous GC analysis of the C_6-montmorillonite complex,[23] the gaseous species evolved in the first step around 300 °C has been identified as n-hexylamine, which indicates the simple deintercalation of amines. This assertion is also supported by the XRD pattern of the sample heated to 310 °C under flowing N_2 (Fig. 7(a)). The XRD pattern for the heated sample reveals a weak superlattice line at $2\theta = 3.91°$ ($d_{001} = 22.6$ Å) due to the 1 : 1 regular interstratification between the 13 Å parallel monolayers and the 9.6 Å silicate layers. The second weight loss step observed at 310–365 °C can be assigned to the decomposition of alkylammonium molecules from the highly charged interlayers. In this stage, however, catalytic alkyl chain cleavage seems to be involved in part since the thermal activation energy for the silicate surface is obtained. Although it is difficult to assign exactly the evolved species because simultaneous breaking of the C–N and C–C bonds is possible, it is likely that when the C–N bonds are broken, then the NH_4^+ ions might be left in the interlayer space. The XRD pattern for the sample heated at 365 °C exhibits a (001) reflection at $2\theta = 8.83°$ ($d_{001} = 10$ Å) (Fig. 7(a)), providing evidence of the formation of an NH_4^+-interlayered silicate.[24] Finally the mass loss beyond 365 °C results from the decomposition of interlayer ammonium cations and some residual carboneous intermediates. The thermal decomposition behavior of the C_8-M hybrid is similar to that described for C_6-M except for an additional weight loss below 250 °C, which can be ascribed to the desorption of C_8 molecules adsorbed excessively between the silicate layers, or in part, loosely attached at edge sites.

For C_{10}- and C_{12}-M hybrids (Fig. 6(a)) with an interstratified structure of 13.8 Å monolayers and 17.9 Å bilayers (Fig. 5(b)), the overall stepwise thermolysis results are very similar. A distinct feature compared to those of C_6- and C_8-M hybrids is a drastic weight loss at around 250 °C. According to the XRD for C_{10}-M hybrid (Fig. 7(b)), the interstratified phase is retained up to 200 °C, beyond which the normal intercalation phase with a parallel monolayer arrangement of alkylammonium molecules prevails. This suggests that the bilayer structure in the mixed layer system turns out to be a monolayer one due to the deintercalation of some of the C_{10} molecules even below 200 °C. Since the monolayer phase remains stable at least up to 250 °C, the drastic weight loss centered at 235 °C (Fig. 6(b)) corresponds to the simple evaporation of desorbed C_{10} molecules from the clay surface. Similarly, the mass loss at 255 °C in C_{12}-M (Fig. 6(b)) is also due to the simple desorption of deintercalated C_{12} molecules. Only the evaporation temperature is slightly higher than that of C_{10}-M due to the higher boiling point of C_{12} (bp = ~248 °C) than C_{10} (bp = ~217 °C). The desorption of alkylammonium molecules from the low-charged layers would occur successively at around 300 °C even though well-defined peaks are not observed in the DTG curves. However, the temperature resolved XRD pattern (Fig. 7(b)) clearly indicates the formation of an interstratified phase between 13 Å layer and 9.6 Å layers as observed in C_6-M after heating at 300 °C. Beyond 300 °C, the thermolysis reaction of C_{10}- and C_{12}-M hybrids follows the pattern observed for C_6- and C_8-M. An additional weight loss at about 430 °C, which becomes enhanced as the number of carbon atoms in the alkyl chain increases, is surely due to the thermal/catalytic breaking of long chain hydrocarbons as reported previously.[23]

For C_{14}- and C_{16}-M hybrids (Fig. 6(a) and (b)), the decomposition of interlayer alkylammonium molecules takes place in three steps. However, the exact assignment of desorption peaks on the basis of layer charge is no longer valid because the discrepancy between the desorption temperature and the evaporation temperature of long chain alkylammonium molecules becomes so large. Actually, the double layer arrangement in the C_{16}-M hybrid is observed to change into a monolayer one even below 250 °C (Fig. 7(c)), although the mass loss occurs rapidly at around 275 °C

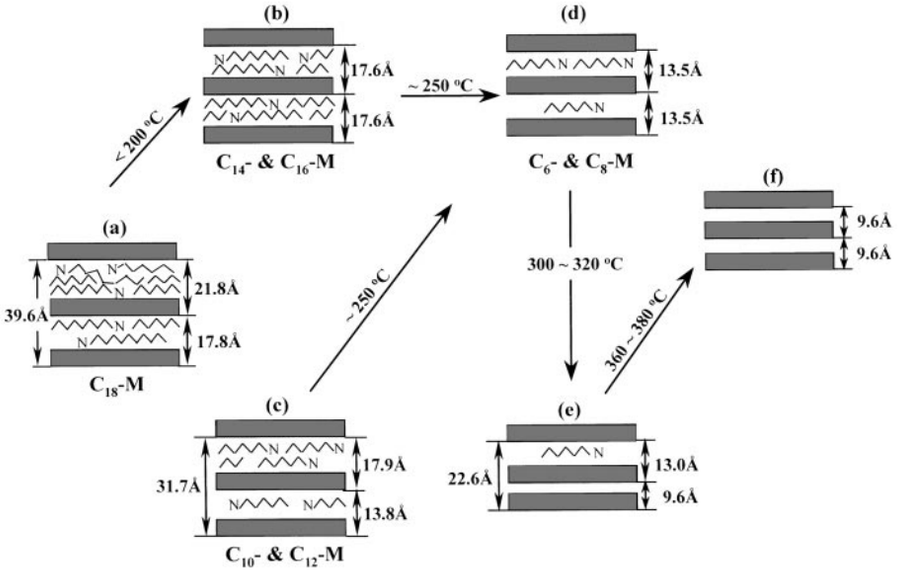

Fig. 8 A stepwise disintercalation of alkylammonium molecules from the silicate layers as a function of temperature.

(Fig. 6(b)). As shown in Fig. 7(c), most of the organic moieties decompose beyond 350 °C.

In C_{18}-M hybrid (Fig. 6(b) and Fig. 7(d)), the interstratified structure of 17.8 Å bilayers and 21.8 Å pseudotriple layers (Fig. 5(d)) is stable up to 200 °C, where some of the C_{18} molecules are deintercalated from the pseudotriple layers, leading to a normal intercalation compound with a basal spacing of 17.6 Å (Fig. 7(d)). Then the bilayer arrangement is again transformed into a monolayer one at about 260 °C (Fig. 7(d)) and subsequently into the interstratified compound of 13.8 Å and 9.6 Å layers along with some 13.8 Å layers at 290 °C (Fig. 7(d)). Finally, the complete decomposition of interlayer species to form 9.6 Å silicate layers is achieved at 380 °C. However the TG loss below 300 °C is small (about 3% of the total weight), indicating that most of the deintercalated C_{18} molecules reside on the clay surfaces until sufficient thermal energy is attained to vaporize and/or to crack the long chain alkylammonium molecules.

Deintercalation pathway

On the basis of the findings from thermogravimetry and temperature-dependent XRD analysis, the possible deintercalation pathways of the alkylammonium-mica hybrids are schematically summarized in Fig. 8. In the interstratified compounds between 17.8 Å bilayers and 21.8 Å pseudotriple layers observed in the C_{18}-M hybrids (a), some of the alkylammonium molecules are desorbed preferentially from the pseudotriple layers below 200 °C to form a normal parallel bilayer arrangement between the silicate layers (b), and the latter phases ((b) and (c)) are subsequently converted into monolayer ones (d) with the desorption of some alkylammonium molecules at around 250 °C. Only beyond the temperature of 300–320 °C does an additional desorption of alkylammonium take place. Since the strength of the electrostatic interaction between alkylammonium molecules and silicate layers is directly influenced by the layer charge density, so the desorption temperature is a measure of the layer charge density of silicates. Therefore, the alkylammonium molecules in the low-charged layers are preferentially deintercalated at this temperature range, which results in the interstratified structure between 13.0 Å monolayers and 9.6 Å silicate layers (e). Finally, the remaining alkylammonium molecules are deintercalated from the highly charged ones at around 360–380 °C to give pristine silicate layers with a basal spacing of 9.6 Å (f). In this case the negative layer charge of the silicate layers would be compensated by the protons provided by the alkylammonium molecule during the desorption.

Conclusion

Layered nano-hybrids of n-alkylammonium intercalated Na^+-fluorine mica are prepared by ion-exchange reaction between the interlayer Na^+ cations and n-alkylammonium cations. According to the observed XRD patterns and their simulation profiles of the organo-mica hybrids, it is found that synthetic Na^+-fluorine mica consists of regularly alternating 1 : 1 layers with high ($\xi_{avg}=0.37$ e^-/Si_4O_{10}) and low layer charge ($\xi_{avg}=0.28$ e^-/Si_4O_{10}). Regularly ordered interlayer stacking along the *c*-axis leads to the formation of interstratified organo-mica nano-hybrids depending upon the number of carbon atoms in the alkylammonium chain. Furthermore, the interlayered gallery species are deintercalated stepwise during thermolysis, reflecting the charge heterogeneity from interlayer to interlayer.

Acknowledgements

This work was supported by the Ministry of Science and Technology (MOST) through the National Nanohybrid Materials Laboratory of NRL Project '99, and J. H. Yang thanks the Ministry of Education through the BK21 fellowship.

References

1 B. M. Barrer, *Zeolites and Clay Minerals as Sorbents and Molecular Sieves*, Academic Press, London, 1978.
2 B. K. G. Theng, *The Chemistry of Clay–Organic Reactions*, John Wiley & Sons, New York, 1974.
3 A. Vaccari, *Appl. Clay Sci.*, 1999, **14**, 161.
4 M. Ogawa and K. Kuroda, *Bull. Chem. Soc. Jpn.*, 1997, **70**, 2593.
5 E. P. Giannelis, *Adv. Mater.*, 1996, **8**, 29.
6 J. H. Choy, S. Y. Kwak, Y. S. Han and B. H. Kim, *Mater. Lett.*, 1997, **33**, 143.
7 G. Lagaly, *Layer Charge Determination by Alkylammonium Ions*, in *Charge Characteristics of 2 : 1 Clay Minerals, the Chemistry of Clay-Organic Reactions*, CMS Workshop 6, ed. A. Mermut, The Clay Mineral Society, Boulder, CO, USA, 1994, pp. 1–46.
8 H. Tateyama, S. Nishimura, K. Tsunematsu, K. Jinnai, Y. Adachi and M. Kimura, *Clays Clay Miner.*, 1992, **8**, 241.
9 H. Tateyama, K. Tsunematsu, H. Noma and Y. Adachi, *J. Am. Ceram. Soc.*, 1996, **79**, 3321.
10 H. Tateyama, H. Noma, S. Nishimura, Y. Adachi, M. Ooi and K. Urabe, *Clays Clay Miner.*, 1998, **46**, 245.

11 K. Urabe, I. Kenmoku and Y. Izumi, *J. Phys. Chem. Solids*, 1996, **57**, 1037.
12 K. Tamura and H. Nakazawa, *Clays Clay Miner.*, 1996, **44**, 501.
13 H. Tateyama, *Finechemical (Japanese)*, 1991, **20**(14), 5–15.
14 T. Kakinoki and Y. Komura, *Acta Crystallogr.*, 1965, **17**, 579.
15 M. Sato, *Clay Sci.*, 1987, **7**, 41.
16 T. Iwasaki and T. Watanabe, *Clays Clay Miner.*, 1988, **36**, 73.
17 H. Tateyama, S. Nishimura, K. Tsunematsu and M. Kimura, *Clay Sci.*, 1992, **8**, 241.
18 G. Rytwo, C. Serban, S. Nir and L. Margulies, *Clays Clay Miner.*, 1991, **39**, 551.
19 G. Lagaly and A. Weiss, *Proc. Reunion Hispano-Belga de Minerales de la Arcilla, Madrid*, 1970, p. 179.
20 G. Lagaly, *Clay Miner.*, 1981, **16**, 1.
21 M. J. Wilson, *A Handbook of Determinative Methods in Clay Mineralogy*, Chapman and Hall, New York, 1987, p. 258.
22 A. Streitwieser, C. H. Heathcock and E. M. Kosower, *Introduction to Organic Chemistry*, 4th edn., Macmillan, New York, 1992, p. 75.
23 J. H. Choy and Y. J. Shin, *Bull. Korean Chem. Soc.*, 1986, **7**, 154.
24 J. Chaussiden and R. Calvet, *J. Phys.Chem.*, 1965, **69**, 2265.